Article type : Technical Note

An Investigation of Errors in Distributed Models' Stream Discharge Prediction Due to Channel Routing

Mohamed ElSaadani, Witold F. Krajewski, Radoslaw Goska, and Michael B. Smith

Research Engineer (**ElSaadani**), Institute for Coastal and Water Research, University of Louisiana at Lafayette, 635 Cajon Dome Blvd., Lafayette, Louisiana 70506; Professor (**Krajewski**) and Staff Engineer (**Goska**), IIHR—Hydroscience & Engineering, University of Iowa, Iowa City, Iowa 52242; and Research Hydrologist (**Smith**), Analysis and Prediction Division, National Weather Service Office of Water Prediction, Silver Spring, Maryland 20910 (E-Mail/ElSaadani: mohamedali-elsaadani@uiowa.edu).

ABSTRACT: Over the summer of 2015, the National Water Center (NWC) hosted the National Flood Interoperability Experiment (NFIE) Summer Institute. The NFIE organizers introduced a national scale distributed hydrologic modeling framework that can provide flow estimates at around 2.67 million reaches within the continental United States. The framework generates discharges by coupling a given Land Surface Model (LSM) with the Routing Application for Parallel Computation of Discharge (RAPID). These discharges are then accumulated trough the National Hydrography Dataset Plus (NHDPlus) stream network. The framework can utilize a variety of LSMs to provide the runoff maps to the routing component. The results obtained from

this framework suggested that there still exists room for further enhancements to its performance, especially in the area of peak timing and magnitude. The goal of our study is to investigate a single source of the errors in the framework's discharge estimates, which is the routing component. The authors substitute RAPID which is based on the simplified linear Muskingum routing method by the non-linear routing component the Iowa Flood Center (IFC) have incorporated in their full hydrologic Hillslope-Link Model (HLM). Our results show improvement in model performance across scales due to incorporating new routing methodology.

(**KEY TERMS**: surface water hydrology; NFIE; runoff; rivers/streams; NHDPlus Dataset.)

Introduction

Floods result from complex interactions between rainfall and several other processes occurring in the atmosphere and landscape. Accurate quantification and prediction of stream discharges is a challenging topic that the hydrologic research community has been trying to overcome for decades. Over the summer of 2015, the National Water Center (NWC), located in Tuscaloosa, Alabama, USA, launched the National Flood Interoperability Experiment (NFIE) Summer Institute, a summer workshop that allowed participants (mainly graduate students) to experiment with research topics related to national flood estimation and forecasting, ranging from runoff generation and discharge estimation to digital inundation mapping and flood risk management. The first author participated in NFIE 2015 and evaluated the performance of the NFIE-Hydro framework, a hydrologic modeling framework that can provide nationwide stream flow estimates in the United States.

In this article, we build on this effort by identifying possible ways to improve the NFIE-Hydro framework (Maidment, 2016). The NFIE-Hydro framework consists of a combination of a runoff-generating Land Surface Model (LSM), Noah Multi-Parameter (Noah-MP) LSM (Niu *et al.,* 2011), and the runoff discharge routing component called the Routing Application for Parallel Computation of Discharge (RAPID) (David *et al.,* 2011). It is also simple to incorporate the runoff estimates from other LSM's, such as or the Variable Infiltration Capacity (VIC) (Xia *et al.,* 2012a, b) as a substitute to the runoff estimates from Noah-MP. Previous studies evaluated the VIC-RAPID combination (e.g., David *et al.,* 2013; 2015; Tavakoly *et al.,* 2016) over multiple regions in the United States. In addition, studies (e.g., David *et al.,* 2011; 2013)

evaluated the accuracy of stream discharge estimates resulting from different LSMs (e.g., VIC, Noah LSM) when combined with RAPID. A recent study presented in Zhao *et al.,* (2017) showed that the choice of the routing component could make a great impact on the performance of the simulated monthly and daily discharges of multiple Global Hydrological Models (GHMs). In this study, however, we restrict our focus to studying the contribution of the routing component to the quality of the discharge estimates in hourly scale over the US. We do so by using the same runoff estimates from the VIC LSM to derive two routing components in a controlled environment that ensures that the differences in the stream flow estimates result from the routing components alone. The two routing components are RAPID, and the routing component developed by the Iowa Flood Center (IFC) and implemented in the full IFC in-house hydrologic model called the Hillslope-Link Model (HLM) (Small *et al.*, 2011; Ayalew *et al.*, 2014; Krajewski *et al.*, 2016).

In this article, we do not intend to compare the routing components as software packages, which would require including other aspects (e.g., computational time and ease of implementation in different study areas etc.), however, previous studies investigated these issues (e.g., David *et al.*, 2016 for RAPID; and Small *et al.*, 2011 for the HLM). The routing methodologies incorporated in the routing components are, the simplified linear Muskingum routing method in the case of RAPID (Cunge, 1969; David *et al.*, 2011), and the non-linear routing methodology based on the power law relationship between the stream discharge and mean flow velocity, and the network hydraulic geometry self-similarity assumption described in Mantilla *et al.*, 2005 and Mantilla 2007.

We tested both routing components' performances over the Cedar River basin, an average sized basin located in eastern Iowa. The basin covers approximately 16,862 km^2, and is monitored by about 11 United States Geological Survey (USGS) gauges. To conduct a fair comparison, we used the same stream flowline and sub-catchment geometries provided by the National Hydrography Dataset Plus Version 2 (NHDPlus V2). The common runoff input obtained from the VIC model has a spatial resolution of 1/8°*1/8° and a temporal resolution of 1 hour. We used the model outputs provided by NASA's Hydrology Data and Information Services Center (HDISC) available at (http://disc.sci.gsfc.nasa.gov/hydrology/data-holdings). The VIC model is widely used and has been extensively evaluated in the past, it provides

advanced capabilities in terms of runoff production such as variable infiltration capacity curves and baseflow conceptualization (Tavakoly *et al.*, 2016; Xia *et al.*, 2012a). We followed the same runoff-routing coupling process explained in Tavakoly *et al.* (2016). Our results show an improvement in the streamflow estimates, especially in the aspects of peak timing and magnitude, due to the implementation of the new routing methodology.

Methods

Hydrologic routing is an approximation of the one-dimensional Saint-Venant equation that involves ignoring the discharge momentum term of the equation, such as the Muskingum method described in Cunge (1969), or the Nonlinear Cascade Reservoir method described in Kim and Georgakakos (2014). On the other hand, some hydrologic routing methodologies use a simplified version of the Momentum equation such as the Muskingum-Cunge described in Cunge (1969) or the non-linear method presented in Mantilla (2007) based on scale invariance and network hydraulic geometry self-similarity.

In this article, we are going to compare two hydrologic routing methods, the Muskingum method and the method presented in Mantilla (2007). An important aspect of this study is that it compares two hydrologic routing methods using the same input from the widely used LSM VIC, in a controlled environment where the runoff amounts ingested into the sub-catchments of each routing component are identical. This ensures that the discrepancies in the discharge estimates obtained from the routing components are strictly due to the difference in the routing methodologies they utilize. In the next two subsections, we provide a brief description of these routing components we use in this study and the methods they utilize.

The RAPID stream flow routing component

The Muskingum method incorporated in RAPID is a one-dimensional diffusion wave approximation of stream discharge based on the continuity equation that ignores the momentum equation; in other words, it is a storage-based equation. The equation depends on two parameters: a storage constant k that has a dimension of time, and x, a dimensionless weighting parameter based on the relative influence of the inflow and outflow. As described in David *et al.*, (2011a), the finite difference form of the Muskingum method is

$$q_i(t+\Delta t) = c_1\left[q_i^{up}(t+\Delta t) + q_i^{e}(t+\Delta t)\right]$$

$$+c_2\left[q_i^{up}(t) + q_i^e(t)\right] + c_3 q_i(t) \quad (1)$$

where,

$$c_{1i} = \frac{\frac{\Delta t}{2} - k_i x_i}{k_i(1 - x_i) + \frac{\Delta t}{2}}, \quad (2)$$

$$c_{2i} = \frac{\frac{\Delta t}{2} - k_i x_i}{k_i(1 - x_i) + \frac{\Delta t}{2}}, \quad (3)$$

and

$$c_{3i} = \frac{k_i(1 - x_i) - \frac{\Delta t}{2}}{k_i(1 - x_i) + \frac{\Delta t}{2}}, \quad (4)$$

For any reach index i, $C_{1i} + C_{2i} + C_{3i} = 1$. In equation 1, q_i is the outflow of a reach i; q_i^e is the lateral flow within a reach i (surface and subsurface); q_i^{up} is the inflow to the reach from upstream links; and t, Δt are the simulation time and the time step, respectively. The output flows from RAPID are affected by the fact that the Muskingum method assumes a uniform water surface profile between the upstream and downstream ends of a channel reach. Also, obtaining accurate k and x values is a difficult task that often includes calibration and optimization by using observations and is dependent on the calibration dataset. The RAPID routing component has an option to optimize the parameters k and x based on available USGS gauge observations. In this study, we used the calibrated k and x dataset available at Tavakoly (2017; Zenodo. DOI: 10.5281/zenodo.322886) and described in Tavakoly *et al.*, (2016). RAPID assumes that the lateral flow q^e enters the channel instantly at the upstream junction of the stream. Lastly, the common approach for handling the runoff maps using RAPID (e.g. David *et al.*, 2011, 2013, 2015, 2016; Tavakoly et al, 2016) lumps surface and subsurface runoff estimates from the LSM and routs them into the stream channels simultaneously.

The HLM routing component

The HLM routing is based on the method presented in Mantilla (2007) where the velocity in the channel element can be obtained using a nonlinear power law relationship with the upstream served area and the stream discharge (similar to that by Paik and Kumar (2004)), where the velocity corresponding to a certain discharge q can be described as

$$v(q) = v_0 {q_{link}}^{\lambda_1} A^{\lambda_2} \quad (5)$$

Consequently, the flow transport equation can be described as follows:

$$\frac{dq_{link}(t)}{dt} = \frac{v_0 q_{link}^{\lambda_1}(t) A^{\lambda_2}}{(1-\lambda_1)l}[$$

$$a_h\left(q_{surf}(t) + q_{subsurf}(t)\right)$$

$$-q_{link}(t) + q_{up}(t)] \quad (6)$$

where q_{link} and q_{up} are the output discharges from a link and inflow from upstream links at time t; A is the total upstream area draining into the hillslope; a_h and l are the hillslope area and length, respectively; and λ_1, λ_2 and v_0 are global parameters of the water velocity component in the model and are set to $0.2, -0.1$ and 0.3, respectively. The parameter estimation for HLM is performed using the power law relationship between channel velocity, discharge and upstream areas at unregulated USGS stream gauges across Iowa, this process doesn't include optimization based on observed hydrographs as a training set. More on how to estimate these parameters and how they vary across geographic locations in the United States Midwest can be found in Mantilla (2007) and (Ghimire *et al.*, "A Power Law Model for River Water Velocity in U.S. Upper Midwestern Basins." Unpublished manuscript, 2017). In this article, the surface and subsurface runoff estimates, q_{surf} and $q_{subsurf}$ consequently, are lumped prior to routing in a similar fashion to RAPID. We matched our model setup to that used to prepare the RAPID parameters' values to ensure fair comparison. However, we conduct our comparisons at a mid-sized basin included in this domain because it is well monitored with USGS stream gauges across a wide range of scales. In addition, the effect of artificial storage in this basin is negligible. It is also important to note that the estimation of the HLM model parameters is independent of the rainfall-runoff model's input, Mantilla (2007).

Evaluation procedure

We conduct our evaluation at the Cedar River basin, which is located in eastern Iowa. The Cedar River Basin has a drainage area of 16,814 km^2. Eleven USGS gauges monitor the area and cover a range of scales (from 776 km^2), and are not affected by river regulation. The USGS gauge locations are shown in Figure 1 and the areas they serve are listed in the legend. Our study period is the warm season (May through September) of 2014. We allowed a two-

month spin-up period (runs started on March 1st) and proper initialization for both models. Both simulated and observed discharges used in this study have an hourly temporal resolution.

We calculate three statistical skill scores at each gauge location, the percent Root Mean Square Error RMSE, correlation coefficient, and Nash-Sutcliffe efficiency (NSE). The reader is encouraged to review Moriasi *et al.,* (2007) and Tavakoly *et al.,* (2016) to learn more about model's performance classifications based on NSE, RMSE, and Correlation Coefficient performance categories. The equations used to calculate these scores are as follows:

$$\%\, RMSE = \sqrt{\frac{\sum_1^n (q_{sim}^t - q_{obs}^t)^2}{n}} \cdot \frac{1}{max\,(q_{obs})} . 100 \quad (7)$$

$$Corr = \frac{E[(q_{obs} - \mu_{obs})(q_{sim} - \mu_{sim})]}{\sigma_{obs}\, \sigma_{sim}} \quad (8)$$

$$NSE = 1 - \frac{\sum_{t=1}^n (q_{obs}^t - q_{sim}^t)^2}{\sum_1^n (q_{obs}^t - \bar{q}_{obs})^2} \quad (9)$$

In order to better assess the performance of both models in detecting peak times and magnitudes we calculated the hit rate (HR), false alarm ratio (FAR) and the critical success index (CSI) at each station using the 2- year return period peak discharges provided by Eash *et al.,* (2013). Unfortunately, these records are not available at all stations due to lack of sufficient stream discharge records. Only one station out of our eleven stations (station number 7) has an insufficient peak discharge record. The formulas we used to calculate HR, FAR and CSI are as follows:

$$HR = \frac{a}{a+c} \quad (10)$$

$$FAR = \frac{b}{a+b} \quad (11)$$

$$CSI = \frac{a}{a+b+c} \quad (12)$$

where *a* is the instances where the discharge exceeded a certain threshold in both model estimates and observed flow; *b* is when the model estimates exceed the threshold but the observed flow is lower than this threshold; and *c* is when the observed flow exceeds the threshold but the model estimates do not. All these parameters are calculated based on hourly discharges. In short, HR represents the instances when the model predicted that the flow would exceed a certain threshold correctly (ranges from zero (Poor) to one (Good)). FAR represents the instances when the model overestimated the discharge and exceeded a certain threshold (ranges from zero (good) to one (Poor)). CSI, also known as threat score, represents how well the exceeding events of the model correspond to those of the observations by accounting for the incorrect modeled exceedances in the denominator (ranges from zero (Poor) to one (Good)).

In addition, we calculated the difference in time to peak ΔT^p and percent difference in peak discharge ΔQ^p as defined in Vergara *et al.,* (2016), where, as shown in (13) the difference in peak time will be negative in case the simulated peak ($T^p_{simulated}$) occurs ahead of the observed peak ($T^p_{observed}$), but positive in case the simulated peak occurs after the observed peak. Similarly, from (14) the percent difference in peak magnitude will have a positive sign in case the simulated peak ($Q^p_{simulated}$) is greater in value than the observed peak and a negative sign in case the simulated peak is smaller in value than the observed peak ($Q^p_{observed}$).

$$\Delta T^p = T^p_{simulated} - T^p_{observed} \tag{13}$$

$$\Delta Q^p = (Q^p_{simulated} - Q^p_{observed}) / Q^p_{observed} * 100 \tag{14}$$

Results

We begin our comparison between the routing components by visually inspecting the hydrographs presented in Figure 2. The red hydrographs correspond to the VIC-HLM combination, the blue hydrographs correspond to the VIC-RAPID combination, and finally the black hydrographs correspond to the USGS observations. When available, the return period peak discharges are represented by horizontal gray lines on top of the hydrographs (two-year peak discharge is always represented by the lowest gray line above it is the five-year peak discharge and the highest gray line is the ten-year peak discharge). Two main peaks characterize

the observed flow of the year 2014; the first took place around mid-June and the second around early July. A major characteristic of the simulated discharges is that they consistently underestimate the peak discharges in many of the stations, especially during the mid-June event. Since both routing components receive the same runoff estimates and the runoff is eventually routed through the channels; the LSM VIC seems to be a major contributor to this underestimation in the overall water volume. This is supported by the results presented in ElSaadani and Krajewski (2017), where the Noah-MP runoff estimates were used as input for the HLM routing component using the same parameter configuration. The results show improved peak magnitude estimates when Noah-MP runoff is used. An important feature of the VIC-RAPID hydrographs is that they exhibit a flashy behavior, which is dampened as the basin scale increases. This flashy behavior is mainly due to the linear routing method incorporated in RAPID (simplified Muskingum) in comparison to the non-linear routing method incorporated in the HLM routing component.

In Figure 3 we present the statistical skill scores of the routing components spatially over the stream network. The right column shows the skill scores of the HLM routing, while the left column shows the RAPID skill scores. The top row shows the comparison of the correlation coefficients between the simulated and observed hydrographs, while the middle and bottom rows show the % RMSE and NSE comparisons, respectively. These results show that the HLM routing components resulted in an improved simulated discharge estimates across scales (higher correlation and NSE, and lower % RMSE). We included a summary of these skill scores in Table S1. By looking at Table S1, one can infer that the non-linear routing exhibits a more stable performance across different locations (lower standard deviation, SD) with a better overall performance compared to linear routing. In Figure S1 we plotted the skill scores (y-axis) against basin scale (x-axis). The results show that the performance of both routing components improves with increasing basin scale; however, this improvement in performance is more significant for RAPID.

So far, we have evaluated the time series of discharges as a whole, without details about the performance of the routing components during extreme events. Hence, we evaluated indices such as HR, FAR and CSI at all station locations as well as the difference in time-to-peak and percent difference in peak magnitude. We start by comparing the HR, FAR and CSI scores at

each location. Due to the overall underestimation in the simulated peak discharges caused by the LSM, the simulated discharges rarely reached the 5- and 10-year return periods, which is not the case in the observed flow. Thus, the scores estimates for the 5- and 10-year return period are not presented. Figure 4 shows the estimates for the 2-year return period, where the red bars represent the HLM routing component while the blue bars represent the RAPID component. The HLM routing component outperformed the RAPID component by having higher 2-year HR and CSI values, and lower FAR values.

Both routing components experienced an improvement in peak timings and magnitudes across scales during the early July peak. In order to have a better idea about the performance in peak time and magnitude we calculated ΔT^p and ΔQ^p for each peak at all station locations. Table 1 contains the outcome of this analysis where the left panel of the table compares the performance of the routing components during the mid-June peak (Event 1), and the right panel for the performance of the routing components during the early July event (Event 2). The summary of statistics at the bottom four rows of the table shows that for the first peak, although both routing components seem to have placed the peaks ahead of time, RAPID estimates experienced a much earlier peak time when compared to the observed peak. On average, both routing components underestimated the peak magnitudes, however, with a higher variability (standard deviation) in the case of RAPID due to its flashy behavior. Both routing components performed much better in estimating the second peak timing with similar standard deviation of peak time errors. Nevertheless, the HLM underestimated the peak magnitudes and RAPID overestimated them, with greater variance in case of RAPID.

Conclusions and Recommendations

The main goal of this study is to highlight the contribution of the stream discharge routing methodologies to the errors in simulated stream discharge estimates. We observed that the routing methodology have a significant impact on our hydrologic model's performance. This difference in performance generally decreases as the basin scale increases. As expected, the linear Muskingum method resulted in a flashy behavior in the simulated discharges, especially in smaller basin scales. The non-linear routing method incorporated in the HLM routing component resulted in improved discharge estimates characterized by better peak times and magnitudes. It is evident that a major contributor to the errors in the estimated discharges is the

LSM runoff estimates, which in turn will have an effect on the routing components performance, since all the velocities in the streams are determined by the amount of runoff available in their served area. However, determining the amount of error caused by the LSM is not our focus in this study. Future recommendations for this study include, first, expanding the study domain to include a wider range of scales and different hydro-climatic regions. This however may require implementing reservoir operation in the routing components in order to have a fair comparison with the observed discharges. Second, evaluating the HLM routing component with runoff estimates from a variety of LSMs. Finally, a more comprehensive technique of estimating the peak time difference based on Continuous Wavelet Transform, which also accounts for peak magnitude and range, is described in ElSaadani and Krajewski (2017). We hope that our study will be followed by many similar investigations by others in different parts of the country and collectively will contribute to improve national flood estimation and forecasting platforms.

Supporting Information

Additional supporting information may be found online under the Supporting Information tab for this article: Statistical skill scores summary table and performance versus score figures.

Acknowledgments

We gratefully acknowledge the financial support from UCAR's COMET outreach program, grant no. Z16-23476. The authors also thank the organizers of the NFIE summer institute for providing a friendly and collaborative research environment for young scientists. In addition, we would like to thank Prof. Ricardo Mantilla from the Iowa Flood Center for his valuable comments towards the completions of this research.

Literature Cited

Ayalew, T. B., W. F. Krajewski, R. Mantilla, and S. J. Small, 2014. Exploring the Effects of Hillslope-Channel Link Dynamics and Excess Rainfall Properties on the Scaling Structure of Peak-Discharge. *Advances in Water Resources,* 64, 9-20, DOI: 10.1016/j.advwatres.2013.11.010.

Cunge, J. A., 1969. On the Subject of a Flood Propagation Computation Method (Muskingum Method). *Journal of Hydraulic Research*, 7(2), 205-230.

David, C. H., D. R. Maidment, G. -Y. Niu, Z.- L. Yang, F. Habets, and V. Eijkhout, 2011. River Network Routing on the NHDPlus Dataset. *Journal of Hydrometeorology*, 12, 913-934, DOI: 10.1175/2011JHM1345.1

David, C. H., Z. L. Yang, and J. S. Famiglietti, 2013. Quantification of the Upstream-to-Downstream Influence in the Muskingum Method and Implications for Speedup in Parallel Computations of River Flow, *Water Resources Research*, 49, 2783-2800, DOI: 10.1002/wrcr.20250.

David, C.H., J.S. Famiglietti, Z.-L. Yang, and V. Eijkhout, 2015. Enhanced Fixed-Size Parallel Speedup with the Muskingum Method Using a Trans-Boundary Approach and a Large Sub-Basins approximation. *Water Resources Research*, 51(9), 1-25, DOI: 10.1002/2014WR016650.

David, C.H., J.S. Famiglietti, Z.-L. Yang, F. Habets, and D.R. Maidment, 2016. A Dcade of RAPID – Reflections on the Development of an Open Source Geoscience Code. *Earth and Space Science*, 3, 1-19, DOI: 10.1002/2015EA000142.

Eash, D.A., K.K. Barnes, and A.G. Veilleux, 2013. Methods for Estimating Annual Exceedance-Probability Discharges for Streams in Iowa, Based on Data through Water Year 2010: U.S. Geological Survey Scientific Investigations Report 2013-5086, 63 p. with appendix, http://pubs.usgs.gov/sir/2013/5086/.

ElSaadani, M., and F.W. Krajewski, 2017. A Time-based Framework for Evaluating Hydrologic Routing Methodologies Using Wavelet Transform. *Journal of Water Resource and Protection (JWARP)*, 9, 723-744.

Zhao, F. *et al.*, 2017. The critical role of the routing scheme in simulating peak river discharge in global hydrological models. *Environmental Research Letters*, 12, 075003, DOI: 10.1088/1748-9326/aa7250.

Kim, D.H., A.P. Georgakakos, 2014. Hydrologic Routing Using Nonlinear Cascaded Reservoirs. *Water Resources Research*, 50 (8), 7000-7019. DOI: 10.1002/2014wr015662.

Krajewski, W.F., D. Ceynar, I. Demir, R. Goska, A. Kruger, C. Langel, R. Mantilla, J. Niemeier, F. Quintero, B. Seo, S. Small, L. Weber, and N. Young, 2016: Real-Time Flood Forecasting and Information System for the State of Iowa. *Bulletin of the American Meteorological Society*, DOI: 10.1175/BAMS-D-15-00243.1.

Maidment, D.R., 2016. Conceptual Framework for the National Flood Interoperability Experiment. *Journal of the American Water Resources Association (JAWRA)*, 1-13. DOI: 10.1111/1752-1688.12474.

Mantilla, R., and V. K. Gupta, 2005. A GIS Numerical Framework to Study the Process Basis of Scaling Statistics in River Networks, *IEEE Geoscience and Remote Sensing Letters*, 2(4), 404-408, DOI: 10.1109/LGRS.2005.853571.

Mantilla, R., 2007. Physical Basis of Statistical Scaling in Peak Flows and Stream Flow Hydrographs for Topologic and Spatially Embedded Random Self-similar Channel Networks, *Thesis, University of Colorado.*

Moriasi, D.N., J.G. Arnold, M.W. Van Liew, R.L. Bingner, R.D. Harmel, T.L. Veith, 2007. Model Evaluation Guidelines for Systematic Quantification of Accuracy in Watershed Simulations. *Transactions of the ASABE*, 50 (3), 885-900

Niu, G.-Y., et al. 2011. The community Noah Land Surface Model with Multiparameterization Options (Noah-MP): 1. Model Description and Evaluation with Local-Scale Measurements, *Journal of Geophysical Research*, 116, D12109, DOI: 10.1029/2010JD015139.

Paik, K., P. Kumar, 2004. Hydraulic Geometry and the Nonlinearity of the Network Instantaneous Response. *Water Resources Research* 40, W03602.

Small S. J., L.O. Jay, R. Mantilla, R. Curtu, L. K. Cunha, M. Fonley, and W. F. Krajewski, 2013. An Asynchronous Solver for Systems of ODEs Linked by a Directed Tree Structure. *Advances in Water Resources*, 53, 23-32, DOI: 10.1016/j.advwatres.2012.10.011

Tavakoly, A.A., A. D. Snow, C.H. David, M.L. Follum, D.R. Maidment, and Z.-L. Yang, 2016. Continental-Scale River Flow Modeling of the Mississippi River Basin Using High-Resolution NHDPlus Dataset. *Journal of the American Water Resources Association (JAWRA)* 1-22. DOI: 10.1111/1752-1688.12456.

Tavakoly, A.A., 2017. RAPID Input Files Corresponding to the Mississippi River Basin using the NHDPlus v2 Dataset [Data set]. Zenodo. DOI: 10.5281/zenodo.322886

U.S. Geological Survey, 20150805, USGS NED 1 arc-second n42w091 1 x 1 degree ArcGrid 2015: *U.S. Geological Survey: Reston, VA*, http://ned.usgs.gov/, http://nationalmap.gov/viewer.html

Xia, Y., *et al.*, 2012a. Continental-Scale Water and Energy Flux Analysis and Validation for the North American Land Data Assimilation System Project Phase 2 (NLDAS-2): 1. Intercomparison and Application of Model Products, *Journal of Geophysical Research*,117, D03109, DOI:10.1029/2011JD016048.

Xia, Y., et al. 2012b,Continental-Scale Water and Energy Flux Analysis and Validation for the North American Land Data Assimilation System Project Phase 2 (NLDAS-2): 2. Validation of Model-Simulated Streamflow, *Journal of Geophysical Research*, 117,D03110, DOI:10.1029/2011JD016051.

Tables

Table 1. Summary of peak time differences (Δ T) in hours and percent difference in peak discharges (Δ Q%) for the mid-June (Event 1) and early-July (Event 2) peaks.

Station	Event1				Event2			
	VIC-HLM		VIC-RAPID		VIC-HLM		VIC-RAPID	
	Δ T (h)	Δ Q%	Δ T (h)	Δ Q%	Δ T (h)	Δ Q%	Δ T (h)	Δ Q%
1	1	-17.5	-10	-47.9	12	-43.7	-6	54.6
2	-6	-42.4	-46	-60.0	20	-2.2	34	146.4
3	4	-27.2	-56	19.9	2	-5.1	10	259.1
4	-73	-33.4	-100	48.4	-5	-35.4	-15	1.1
5	-22	-6.8	-108	-15.0	-3	8.3	2	100.4
6	0	-38.8	-31	-52.7	-16	-34.2	4	35.9
7	-2	-36.5	-38	-52.8	-1	-19.1	4	89.3
8	-72	-44.6	-89	12.5	0	-59.9	-12	-44.6
9	-17	-36.6	-54	-48.0	-6	-34.8	-18	-15.5
10	-6	-44.0	-21	50.4	-5	-40.0	-14	7.1
11	-10	-32.8	-41	-40.6	8	-36.8	3	-28.2
Max	4.0	-6.8	-10.0	50.4	20.0	8.3	34.0	259.1
Mean	-18.5	-32.8	-54.0	-16.9	0.5	-27.5	-0.7	55.0
Min	-73.0	-44.6	-108.0	-60.0	-16.0	-59.9	-18.0	-44.6
SD	27.8	11.7	32.1	42.3	9.8	20.5	14.9	89.8

List of Figures

Figure 1. The Cedar River basin located in eastern Iowa. The USGS stream gauges located within the basin are represented by green dots. The USGS code and served area of the gauges is shown in the legend. The stations were numbered in an ascending order in the downstream direction.

Figure 2. Hydrographs at the USGS station locations: the red lines represents VIC-HLM, the blue line represents VIC-RAPID, and the black lines are the observations. The

hydrographs were normalized with the maximum observed discharge at each station. The numbers in the panel labels correspond to the station ranking in Figure 1.

Figure 3. A comparison of the statistical skill scores: top row is % RMSE, the middle row is the correlation, and the bottom row is the NSE, with VIC-RAPID on left column and VIC-HLM on the right column.

Figure 4. Comparison of HR left column, FAR middle column and CSI right column (y axes) at different stations (x axes) between VIC-RAPID and VIC-HLM based on the 2-year return period. Blue bars represent the VIC-RAPID scores and red bars represent VIC-HLM scores. Station numbers (x-axis) follow Figure 1 ranking.

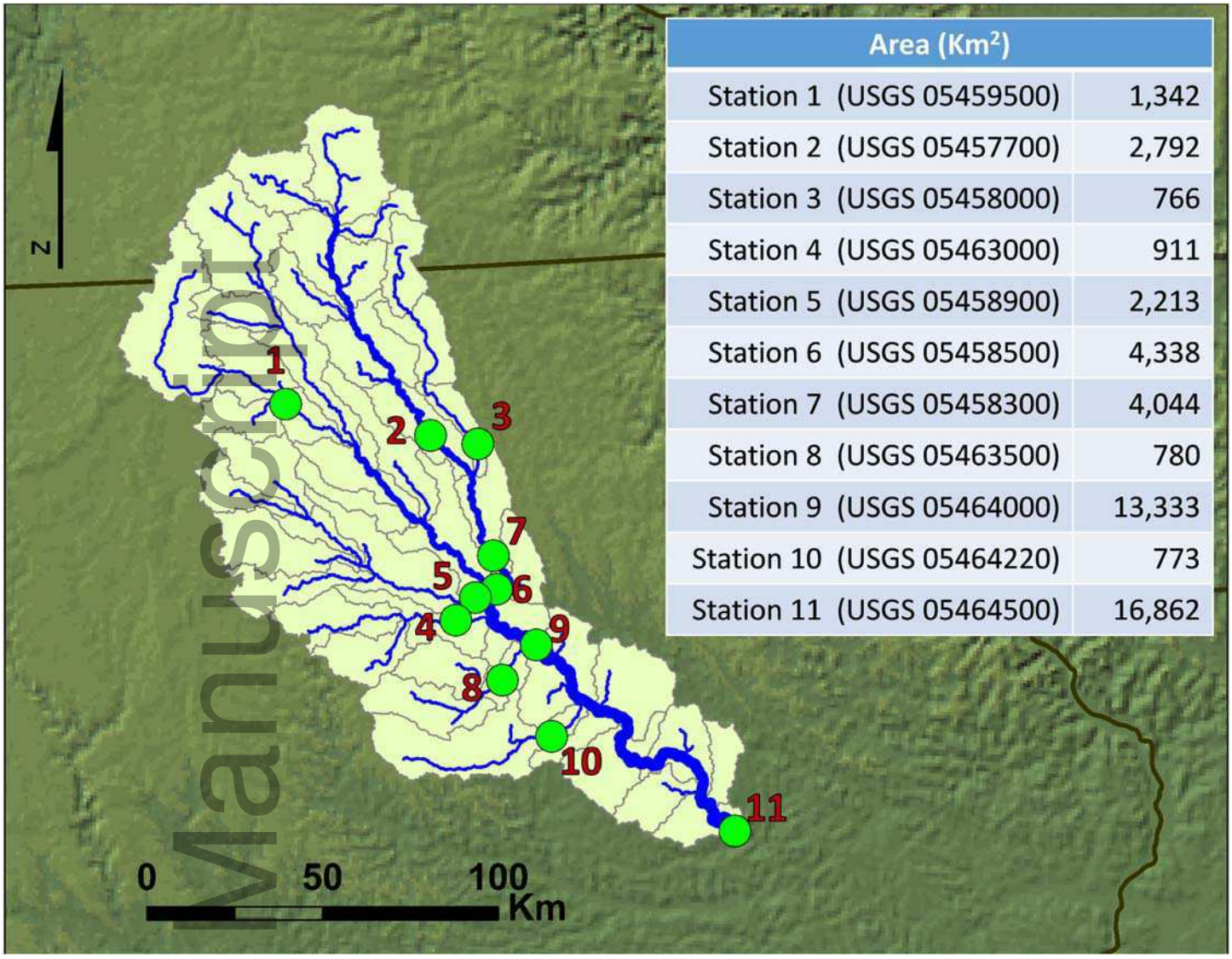

Area (Km^2)	
Station 1 (USGS 05459500)	1,342
Station 2 (USGS 05457700)	2,792
Station 3 (USGS 05458000)	766
Station 4 (USGS 05463000)	911
Station 5 (USGS 05458900)	2,213
Station 6 (USGS 05458500)	4,338
Station 7 (USGS 05458300)	4,044
Station 8 (USGS 05463500)	780
Station 9 (USGS 05464000)	13,333
Station 10 (USGS 05464220)	773
Station 11 (USGS 05464500)	16,862